

# Large-Scale Coherent Dipole Anisotropy ?

S.Basilakos<sup>1,2</sup> & M. Plionis<sup>1</sup>

<sup>1</sup> *National Observatory of Athens, Lofos Nimfon, Thessio, 18110 Athens, Greece*

<sup>2</sup> *Physics Dept., University of Athens, Panepistimiopolis, Greece*

2 October 2018

## ABSTRACT

We have reanalyzed and compared the dipoles of the 1.2 Jy and 0.6 Jy (QDOT) IRAS galaxy samples. We find strong indications from both samples for (a) significant contributions to the gravitational field that shapes the Local Group motion from depths up to  $\sim 170 h^{-1}$  Mpc and (b) a large-scale coherence of the dipole anisotropy, indications provided mainly by the fact that the differential dipoles of large equal volume shells are aligned with the CMB dipole and exhibit significant dipole signals. The two IRAS dipoles are indistinguishable within  $50 h^{-1}$  Mpc and beyond  $\sim 130 h^{-1}$  Mpc while the QDOT dipole, having a lower flux limit, continues growing with respect to the 1.2 Jy sample up to  $\sim 100 h^{-1}$  Mpc in agreement with Rowan-Robinson et al (1990).

**Keywords:** cosmology: observations - galaxies: distances and redshifts - infrared: galaxies - large scale structure of Universe

## 1 INTRODUCTION

The peculiar velocity of the Local Group of galaxies with respect to the Cosmic Microwave Background (CMB) with  $u_{LG} = 622$  km/sec towards  $(l, b) = (277^\circ, 30^\circ)$  is a well established fact (cf. Kogut et al. 1993). The most probable cause for this motion as well as for the observed peculiar motions of other galaxies and clusters (cf. Dekel 1997 and references therein) is gravitational instability (cf. Peebles 1980). This is supported by the fact that the gravitational dipole (acceleration) of many different samples of extra-galactic mass tracers is well aligned with the general direction of the CMB dipole (cf. Yahil, Walker & Rowan-Robinson 1986; Lahav 1987; Lynden-Bell et al 1988; Miyaji & Boldt 1990; Rowan-Robinson et al 1990; Strauss et al 1992; Hudson 1993; Scaramella et al 1991; Plionis & Valdarnini 1991; Branchini & Plionis 1996). However, what still seems to be under discussion is from which depths do density fluctuations contribute to the gravitational field that shapes the Local Group motion. The largest such depth is defined by the dipole *convergence depth*,  $R_{conv}$ , which is that depth where the true gravitational acceleration converges to its final value. The outcome of many studies, using different flux or magnitude limited galaxy samples, is that the apparent value of  $R_{conv}$  differs from sample to sample, in the range from 40 to  $100 h^{-1}$  Mpc, with a strong dependence to the sample's characteristic depth. This

probably implies that the apparent dipole convergence is spurious, due to lack of adequately sampling the distant density fluctuations. Only the optical Abell/ACO cluster sample is volume limited out to a large enough depth ( $\simeq 240 h^{-1}$  Mpc) to allow a more reliable determination of  $R_{conv}$  which was found to be  $\simeq 160 h^{-1}$  Mpc (Scaramella et al 1991; Plionis & Valdarnini 1991; Branchini & Plionis 1996). Recently, this result has been confirmed using X-ray cluster samples, which are free of the various systematic effects from which the optical catalogues suffer (Plionis & Kolokotronis 1998).

If there is a linear bias relation between the cluster, the galaxy and the underlying matter density fluctuations, as usually assumed (cf. Kaiser 1984), then the galaxy dipole should also have similarly deep contributions. In this study we reanalyse the 1.2 Jy and the deeper QDOT 0.6 Jy IRAS galaxy dipoles, initially investigated by Strauss et al (1992) and Rowan-Robinson et al (1990) respectively, with the aim of investigating whether there are any such indications.

## 2 IRAS GALAXY SAMPLES AND SELECTION FUNCTIONS

We use in our analysis the two available flux-limited 60- $\mu$ m IRAS samples; one limited at  $S_{lim} = 1.2$  Jy (Fisher et al 1995) and the other at  $S_{lim} = 0.6$  Jy (Rowan-

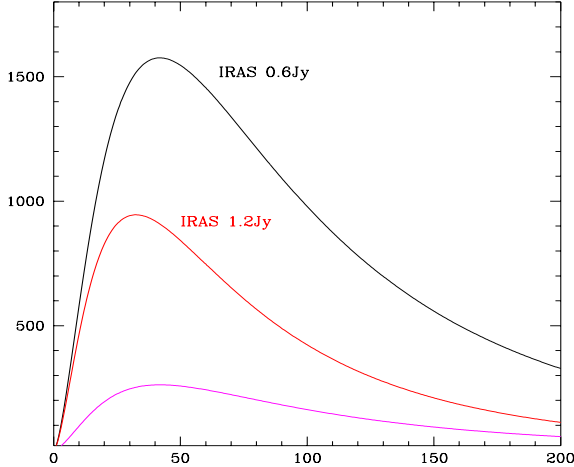


**Figure 1.** The expected  $N(r)$  distribution, according to the IRAS galaxy luminosity function, for the 1.2 Jy, the QDOT 0.6 Jy and the PSCz 0.6 Jy IRAS samples.

Robinson et al 1990), which has a 1 in 6 sampling rate. The IRAS 1.2 Jy contains 5763 galaxies with  $|b| > 5^\circ$  while the QDOT contains 2086 galaxies with  $|b| > 10^\circ$ . Note that although the two catalogues are not totally independent, a cross correlation revealed only 105 common galaxies (with  $\delta\theta \leq 0.6^\circ$  and  $\delta cz \leq 800$  km/sec).

To estimate the local acceleration field it is necessary to recover the true galaxy density field from the observed flux-limited samples. This is done by weighting each galaxy by  $\phi^{-1}(r)$ , where the selection function,  $\phi(r)$ , is defined as the fraction of the galaxy number density that is observed above the flux limit at some distance  $r$ . Therefore

$$\phi(r) = \frac{1}{\langle n_g \rangle} \int_{L_{min}(r)}^{L_{max}} \Phi(L) dL \quad (1)$$

where  $L_{min}(r) = 4\pi r^2 \nu S_{lim}$  is the luminosity of a source at distance  $r$  corresponding to the flux limit  $S_{lim}$ ,  $\nu = 60\text{-}\mu\text{m}$  and  $\langle n_g \rangle$  is the mean galaxy number density, given by integrating the luminosity function over the whole luminosity range, with  $L_{min} = 7.5 \times 10^7 h^2 L_\odot$  since lower luminosity galaxies are not represented well in the available samples (cf. Rowan-Robinson et al 1990; Fisher et al 1995), and  $L_{max} = 10^{13} h^2 L_\odot$ . Obviously,  $\phi(r)$  is a decreasing function of distance because a smaller fraction of the luminosity function falls above the flux limit at greater distances.

For the QDOT sample we used the Saunders et al (1990) luminosity function while for the IRAS 1.2 Jy we used the parameterised selection function of Yahil et al (1991). We have verified, however, that the two selection functions are indistinguishable from each other when applied to the same flux limit. In figure 1 we present the  $\phi(r)$  of the IRAS 1.2 and 0.6 Jy samples, for the 1-in-6 (QDOT) as well as for the unavailable 6-

in-6 sampling rate (PSCz). It is evident that although the QDOT sample is deeper, it samples the galaxy distribution more sparsely than the 1.2 Jy sample.

### 3 DIPOLE CALCULATION

We determine the peculiar acceleration of Local Group galaxies by measuring moments of the IRAS galaxy distribution. The dipole moment:  $\mathbf{D} = \sum \phi^{-1}(r) r^{-2} \hat{r}$ , is calculated by weighing the unit directional vector pointing to the position of each galaxy, with the gravitational weight of that galaxy and summing over all available galaxies with distances greater than  $5 h^{-1}$  Mpc (on smaller scales the observed galaxies do not adequately represent the true distribution; cf. Rowan-Robinson et al 1990). Similarly the monopole term is:  $M = \sum \phi^{-1}(r) r^{-2}$ .

We then estimate the gravitational acceleration induced on the LG from the distribution of IRAS galaxies by:

$$\mathbf{V}_g(r) = \frac{H_0 R_{conv}}{M(\leq R_{conv})} \mathbf{D}(r) \quad (2)$$

(cf. Miyaji & Boldt 1990; Plionis et al 1993). Using linear perturbation theory (cf. Peebles 1980) and equation (2) we can relate the Local Group peculiar velocity with the estimated acceleration by:

$$\mathbf{u}_{LG}(r) = \beta_I \mathbf{V}_g(r) \quad (3)$$

where  $\beta_I = \Omega^{0.6}/b_I$  and  $b_I$  is the IRAS galaxy to underlying mass bias factor.

#### 3.1 Treatment of the IRAS galaxy data

Due to systematic effects and biases present in the data we have to perform various corrections to the raw dipole estimates. Firstly we need to treat the excluded, due to cirrus emission, galactic plane. We do so by extrapolating to these regions the data from the rest of the unit sphere with the help of a spherical harmonic expansion of the galaxy surface density field and a sharp mask (cf. Yahil et al 1986; Lahav 1987). Secondly, about 4% of the sky is not covered by the catalogue and we apply to these areas a homogeneous distribution of galaxies having the mean weight, estimated from the rest of the sky. Thirdly, due to discreteness effects and the steep selection function with depth we have an additive dipole term, the *shot-noise dipole*, for which we have to correct our raw dipole estimates. Assuming Gaussianity, the Cartesian components of the shot noise dipole are equal ( $\sigma_x = \sigma_y = \sigma_z$ ) and thus  $\sigma_{3D}^2 = 3\sigma_{i,1D}^2$  (cf. Hudson 1993). Taking the coordinate system such that one of the shot-noise dipole components is parallel to the z-axis of the true dipole and we can attempt an approximate correction of the raw dipole according to the following model:

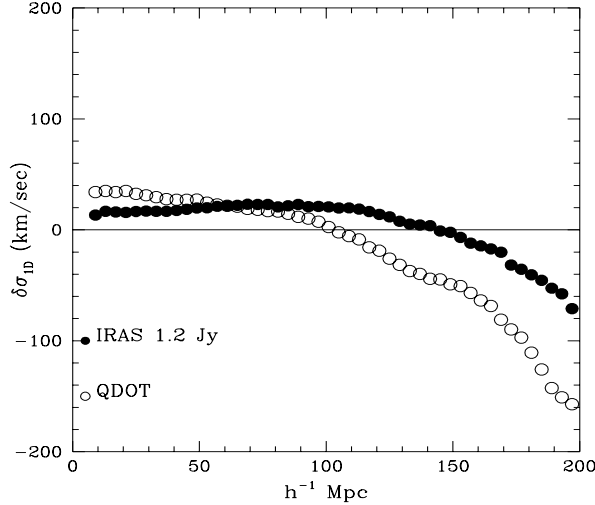


**Figure 2.** Difference between the Monte-Carlo and the Strauss et al (1992) 1-d shot-noise estimates, for both IRAS 1.2 Jy and QDOT samples.

$$D_{cor} = D_{raw} - \sigma_{3D}/\sqrt{3} \quad (4)$$

Note that this correction model although more severe than the usual  $D_{cor}^2 = D_{raw}^2 - \sigma_{3D}^2$  model, it provides qualitatively similar dipole corrections. We choose, however, to use this model in order to be conservative and to obtain a sort of lower limit to the resulting dipole, as far as the shot-noise correction is concerned, and thus via eq.(3) an upper limit to the estimated cosmological  $\beta$  parameter (see section 4.4).

To calculate  $\sigma_{3D}$  we use two methods; a Monte-Carlo simulation approach in which we randomise the angular coordinates of all galaxies while keeping their distance, and thus their selection function, unchanged while the second method is the analytic estimation of Strauss et al (1992):  $\sigma_{3D}^2 \simeq \sum \phi_i^{-1} r_i^{-4} (\phi_i^{-1} + 1)$ . Figure 2 shows the difference (in velocity units) between the two shot-noise estimates. It is evident that the two methods give equivalent results although due to the statistical nature of the first method we believe that it performs better on large depths, where the number density of IRAS galaxies is very low.

### 3.2 $z$ to 3d frame correction

The final but essential correction is to transform redshifts to 3-d distances in order to minimise the so called ‘Kaiser’ effect (Kaiser 1987). This effect can be understood by noting that the distribution of galaxies in redshift space differs from that in real comoving space by a non-linear term:

$$cz = H_0 r + (\mathbf{v}(r) - \mathbf{v}(0)) \cdot \hat{\mathbf{r}} \quad (5)$$

where  $\mathbf{v}(0) (\equiv \mathbf{u}_{LG})$  is the peculiar velocity of the Local Group and  $\mathbf{v}(r)$  the peculiar velocity of a galaxy at position  $\mathbf{r}$ . If  $\mathbf{v}(r)$  had random orientation, then

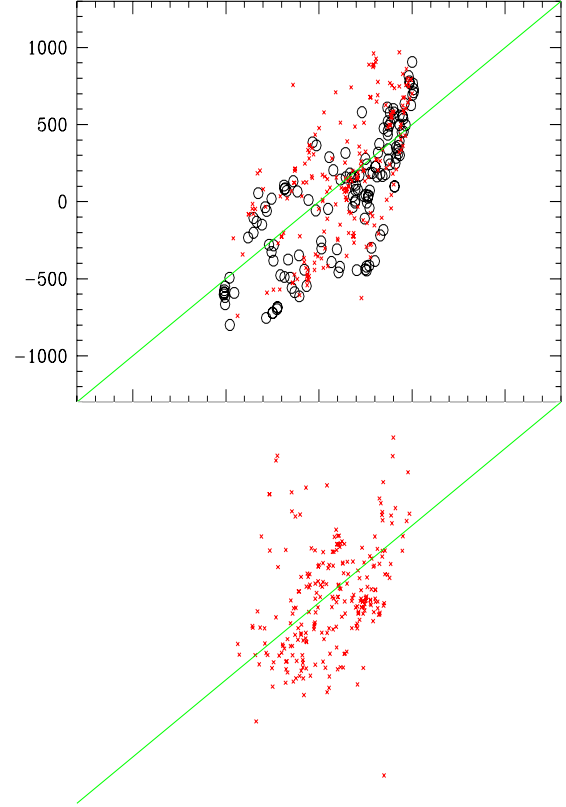


**Figure 3.** Comparison of local 1.2 Jy IRAS galaxy peculiar velocities provided by our model and by the full iterative algorithm within  $cz \sim 3600$  km/sec (see text). The diagonal line corresponds to  $\mathbf{v}_{recons} \cdot \hat{\mathbf{r}} = \mathbf{V}_{bulk} \cdot \hat{\mathbf{r}}$ .

$\int \mathbf{v}(r) \cdot \hat{\mathbf{r}} d^3r \approx 0$  and the last term of eq.(5) is dominated by the LG term; we thus obtain that in the LG frame (ie., when using  $cz = H_0 r$ ), structures in the direction of our motion appear at a redshift smaller than their true distance in the CMB frame and thus they will artificially enhance the amplitude of the gravitational dipole.

However, many studies indicate that local galaxies have peculiar velocities not randomly oriented but rather participating in a coherent flow (bulk motion) together with the Local Group (ie.,  $\mathbf{v}(r) \approx \mathbf{v}(0)$ ) within at least a volume of radius  $\sim 5000$  km/sec (cf. Lynden-Bell et al 1988, Dekel 1994; 1997, Strauss & Willick 1995). If so, it would be reasonable to evaluate the IRAS dipole in the LG frame, since in this case  $cz \approx H_0 r$ . However, this is not absolutely true since there should exist also a velocity component due to the local, non-linear, dynamics acting between nearby galaxies and/or clusters of galaxies. We can therefore view the galaxy peculiar velocities as consisting of two vector components; a bulk flow and a local non-linear term:

$$\mathbf{v}(r) = \mathbf{V}_{bulk}(r) + \mathbf{v}_{nl}(r) \quad (6)$$

Inserting eq.(6) in eq.(5) and assuming that  $\mathbf{v}(r) \cdot \hat{\mathbf{r}} \approx \mathbf{V}_{bulk}(r) \cdot \hat{\mathbf{r}}$ , i.e., that the dominant component is that of the bulk flow <sup>\*</sup> we can use the observed bulk flow profile, as a function of distance, given by Dekel (1994; 1997) and combined with that of Branchini, Plionis & Sciamia (1996) to correct the galaxy redshifts. The zero-point,  $V_{bulk}(0)$ , and the direction of the bulk flow is estimated applying eq.(6) at  $r = 0$  and assuming, due to the ‘‘coldness’’ of the local velocity field (cf. Peebles 1988), that  $\mathbf{v}_{nl}(0) \simeq \mathbf{v}_{inf}$  (where  $v_{inf}$  is the LG infall velocity to the Virgo Supercluster). Using the average value from the literature, i.e.  $v_{inf} \simeq 170$  km/sec, we obtain  $V_{bulk}(0) \simeq 500$  km/sec towards  $(l, b) \simeq (276^\circ, 15^\circ)$ .

We test our model by comparing peculiar velocities that it provides with those resulting from the full dynamical algorithm (kindly provided by Dr. Enzo Branchini) which estimates, using linear theory, the gravitational acceleration at the position of each galaxy and then recovers the real-space galaxy distances by solving iteratively the generalised Hubble law of eq.5 (cf. Yahil et al 1991; Strauss et al 1992). In figure 3 we present this comparison for relatively local galaxies in regions of  $\delta\rho/\rho < 1$  (since at dense regions the non-linear component that we neglect in our model will dominate the galaxy peculiar velocity). We find a good correlation within  $cz \sim 4000$  km/sec which is in fact the region where such corrections can affect the dipole. The correlation, at larger distances, progressively fades away since the bulk flow amplitude is low at such distances and the galaxy peculiar velocities are dominated by the distant *local* dynamics. In any case at such distances we do have  $\int \mathbf{v}(r) \cdot \hat{\mathbf{r}} d^3r \approx 0$  and thus redshift space distortions are dominated by the LG term in eq.(5) for which we do indeed correct the galaxy redshifts. Note that we have verified that the amount of scatter seen in figure 3 is well reproduced from our model if we include a randomly oriented non-linear velocity component with  $\langle (\mathbf{v}_{nl} \cdot \hat{\mathbf{r}})^2 \rangle^{1/2} \approx 320$  km/sec.

We have further tested the robustness of the recovered real-space distribution by performing 200 Monte-Carlo simulations in which we vary  $v_{inf}$  (and therefore also the amplitude and slightly the direction of  $\mathbf{V}_{bulk}(0)$ ) as well as the amplitude of  $V_{bulk}(r)$  for all  $r$ 's, by randomly sampling a Gaussian having as mean ( $\mu$ ) the nominal velocity values and  $\sigma = 2\mu/3$ . Furthermore, we investigate how our results change when using the bulk-flow direction of Lauer & Postman (1994); i.e.,  $(l, b) \simeq (343^\circ, 52^\circ)$  with  $|V_{bulk}(r)| = 650$  km/sec for  $r \leq 130 h^{-1}$  Mpc.

Finally, we would like to point out that it so happens that the IRAS dipole, estimated in either the LG or the CMB frames, which should provide a sort of upper

<sup>\*</sup> in a sense we assume that the vector average of  $\mathbf{v}_{nl}(r) \cdot \hat{\mathbf{r}}$  over a whole sky distribution of galaxies is  $\simeq 0$ ; not an unreasonable assumption in the limit of dense sampling.

and lower dipole bounds respectively, differs very little and thus the  $z$  to  $3d$  frame correction *does not have a major consequence in our main dipole results*. We do however investigate, in section 4.2, possible systematic effects that could be introduced by the frame transformation procedure in our IRAS-CMB dipole alignment results.

## 4 MAIN RESULTS

In figure 4a we present the two IRAS dipoles in redshift space. We observe that they are consistent, although up to  $\sim 50 h^{-1}$  Mpc the 1.2 Jy dipole is systematically higher than the QDOT dipole. However, once we correct for redshift space distortions (figure 4b) the two corrected dipoles almost coincide within  $50 h^{-1}$  Mpc, as they should since both samples, due to their relative low flux limits, are good tracers of the Local Universe. Up to  $\sim 130 h^{-1}$  Mpc the amplitudes of the two real-space dipoles deviate with the QDOT being larger than the IRAS 1.2Jy, which is to be expected since the QDOT sample has a lower flux limit and thus it can ‘see’ the distant matter fluctuations better than the 1.2 Jy sample. Beyond  $\sim 130 h^{-1}$  Mpc, however, the two IRAS dipoles coincide again. As can be seen from figure 4, redshift space distortions enhance significantly the real-space dipole (by  $\sim 12\%$ ) only within  $\sim 50 h^{-1}$  Mpc. The uncertainties of the velocity field model, probed by the Monte-Carlo simulations discussed previously, introduce a small scatter in the real-space dipole as indicated by the errorbars in figure 3b. Using the Lauer & Postman (1994) bulk-flow leaves unaltered our main dipole results with only a small ( $\sim 40$  km/sec) amplitude decrease.

### 4.1 Evidence for $> 100 h^{-1}$ Mpc dipole contributions

Between  $\sim 150 - 180 h^{-1}$  Mpc there is an apparent amplitude bump, seen in both redshift and real-space IRAS dipoles. This bump is accompanied by a  $\sim 5^\circ$  decrease of the misalignment angle between the two IRAS dipoles and that of the CMB, the overall misalignment angles at  $r = 200 h^{-1}$  Mpc being  $\sim 23^\circ$  and  $\sim 35^\circ$  for the 1.2 Jy and QDOT samples, respectively. These facts suggest that this dipole amplitude bump is not due to shot-noise uncertainties but rather it is an intrinsic effect, indicating the existence of contributions to the Local Group motion from such large scales. Such contributions cannot be accurately determined, however, from the present flux-limited samples and deeper samples are required for such a task (see Kolokotronis et al 1996). To further investigate these probable deep IRAS dipole contributions we estimate the differential dipole in large equal volume shells (see Plionis, Coles & Catalan 1993 for an earlier attempt in  $z$ -space). We investi-

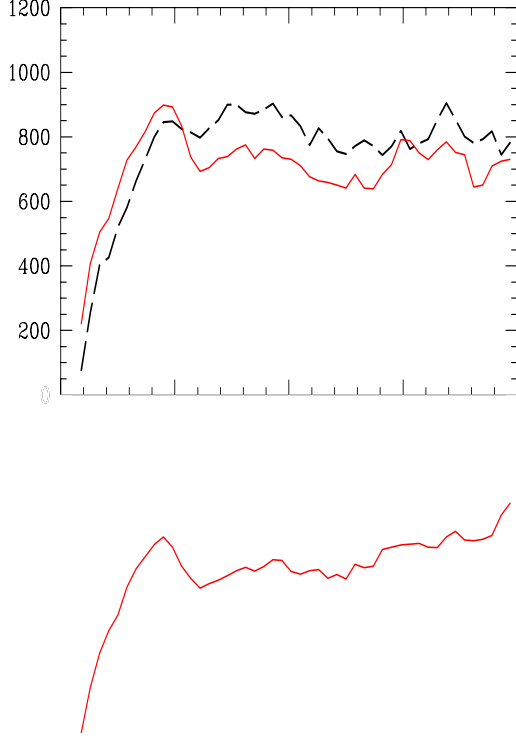


**Figure 4.** (a) IRAS 1.2 Jy (continuous line) and QDOT (dashed line) dipoles in redshift-space. (b) the corresponding dipoles in real-space. The errorbars (shown only for the QDOT dipole) are estimated from Monte-Carlo simulations of the velocity field model (see text).

**Table 1.** Differential 1.2 Jy IRAS dipole directions, the corresponding misalignment angles with respect to the CMB dipole, the dipole signal to noise ratio and probabilities of alignment within  $\delta\theta$  (see text for complete definition). The errorbars are estimated from Monte-Carlo simulations of the velocity field model, with the last two shells having no corresponding uncertainties because we take  $V_{bulk}(r) = 0$  for  $r > 170 h^{-1}$  Mpc (see text).

$h^{-1}\text{Mpc}$	$N_{gal}$	$S/N$	$l^\circ$	$b^\circ$	$\delta\theta_{cmb}$	$p_{mc}$	$p_f$
5-110	4329	$4.7\pm 0.2$	246.0	35.5	$26\pm 3$	0.003	0.051
110-139	390	$0.6\pm 0.2$	311.8	84.1	$55\pm 17$	0.522	0.213
139-159	220	$1.7\pm 0.2$	268.9	8.5	$22\pm 4$	0.026	0.036
159-175	128	$0.6\pm 0.2$	307.1	31.5	$26\pm 7$	0.073	0.051
175-188	72	0.0	96.6	61.4	89	0.655	0.492
188-200	59	1.6	282.8	43.2	14	0.029	0.016

gate shell sizes ranging from  $2.5 \times 10^6$  to  $8.2 \times 10^6 h^{-3}$   $\text{Mpc}^3$  which give qualitatively similar results. In tables 1 & 2 we present the differential dipole directions and misalignment angles with respect to the CMB dipole as well as a measure of the significance of the dipole of each individual shell, given by:

**Table 2.** QDOT dipole results (as in Table 1).

$h^{-1}\text{Mpc}$	$N_{gal}$	$S/N$	$l^\circ$	$b^\circ$	$\delta\theta_{cmb}$	$p_{mc}$	$p_f$
5-110	1267	$2.3\pm 0.2$	232.5	30.3	$38\pm 3$	0.016	0.011
110-139	210	$-0.1\pm 0.2$	98.8	36.6	$113\pm 26$	0.89	0.71
139-159	96	$1.2\pm 0.2$	271.1	-12.7	$43\pm 9$	0.116	0.134
159-175	66	$1.2\pm 0.1$	272.1	31.6	$5\pm 2$	0.004	0.002
175-188	53	-0.9	164.4	-73.7	125	0.55	0.78
188-200	31	0.7	318.4	-15.6	60	0.55	0.25

$$\frac{S}{N} = \frac{D_{raw}}{\sigma_{3D}} \cos(\delta\theta_{cmb}). \quad (7)$$

for the case of  $\delta V \simeq 5.5 \times 10^6 h^{-3} \text{Mpc}^3$  (six shells). We observe that for the QDOT sample there are 3 shells with relatively small misalignment angles and dipole signal to noise ratios  $> 1$ , the deepest shell being [159–175]  $h^{-1}$  Mpc, in which  $\delta\theta_{cmb} \sim 5^\circ$ . For the 1.2 Jy sample, which although shallower has a better sampling, we have small misalignment angles ( $\delta\theta_{cmb} \lesssim 27^\circ$ ) in the same shells but also in a deeper shell (188 – 200  $h^{-1}$  Mpc). Out of these four aligned shells there are significant dipole contributions ( $S/N > 1$ ) only in three while the probability that these alignments are random is extremely low. The formal probability that two vectors are aligned within  $\delta\theta$  is given by the ratio of the solid angle which corresponds to  $\delta\theta$ , to the solid angle of the whole sphere, ie.,  $p_f(\delta\theta) = \sin^2(\delta\theta/2)$ .

We can now estimate the joint probability of alignment, within the observed  $\delta\theta_{cmb}$ , of  $N$  independent vectors, which is given by:

$$P^N \approx \prod_{i=1}^N p_i(\delta\theta)/p_i(90^\circ) \quad (8)$$

Between three shells (first, fourth and sixth) the IRAS galaxy correlation function is zero, due to the large distances involved, and consequently the shells can be considered independent. Due, however, to the vicinity and therefore the possible correlation between the third and fourth QDOT shell we will consider their joint probabilities as limits. Therefore, we have that the joint probability of alignment between the CMB and the differential IRAS equal-volume dipole directions (for those with significant dipole signal  $S/N > 1$ ) is:

$$2 \times 10^{-4} \lesssim P_{\text{QDOT}}^{2,3} \lesssim 8 \times 10^{-4}$$

$$P_{1.2\text{Jy}}^3 \simeq 2 \times 10^{-4}.$$

for the QDOT and IRAS 1.2 Jy samples, respectively.

## 4.2 Test for systematic alignment errors

The observed differential dipole alignments could in principle be due to errors in the correction used to recover the 3-d frame in which we measure the dipole. For example, if redshift errors especially at large distances, were the sampling rate is low, were comparable to a significant fraction of the LG velocity, then using

the 3-d galaxy distances estimated from eqs (5), (6) and  $v(0) = 622$  km/sec, we could artificially produce a false alignment of the distant shells differential dipole with that of the CMB. We therefore address the question of which are the dipole alignments induced totally due to our frame transformation procedure ie., for the extreme case where there is no intrinsic dipole and no LG peculiar velocity. We run 5000 Monte-Carlo simulations in which we destroy the intrinsic IRAS galaxy dipole as well as redshift space distortions by randomising the angular coordinates of the galaxies while keeping their distances and therefore their selection function unchanged. On this intrinsically random galaxy distribution we apply our  $z$  to  $3d$  space transformation and then measure the artificially induced differential dipole alignments due to the frame transformation itself. The coupling between the space distortion and the selection function results in a non-trivial alignment behaviour. In the first shell we observe anti-alignments while at more distant shells the artificial alignment effect does appear. For example at the last shell the median  $\delta\theta$  is  $\sim 67^\circ$  instead of  $90^\circ$ . However, it is impossible to create the observed IRAS dipole alignments if there is no true signal present. We quantify this by measuring the probability,  $p_{mc}(\delta\theta)$ , of observing in our Monte-Carlo simulations dipole alignments as large as the observed IRAS differential dipole alignments. For the shells of interest we find that this probability is low and comparable to the expected  $p_f$ , which implies that the frame transformation uncertainties cannot induce the observed IRAS dipole alignments (see the corresponding values of  $p_{mc}$  and  $p_f$  in the tables).

We conclude that the differential dipole directions are not randomly oriented with respect to the CMB and therefore we do not only have indications for significant dipole contributions from large depths but also for a coherent anisotropy extending to these large scales.

### 4.3 Possible cause of the large-scale IRAS dipole contributions

It is interesting that strong evidence exist for deep dipole contributions from the available galaxy cluster data. Contributions up to  $\sim 20\% - 30\%$  of the total cumulative optical and X-ray cluster dipole, were found from  $\sim 140 - 160 h^{-1}$  Mpc depths (Scaramella et al 1991; Plionis & Valdarnini 1991; Branchini & Plionis 1996; Plionis & Kolokotronis 1998). Similar *coherence* of the differential dipoles in equal volume shells was also found in galaxy cluster case (Plionis & Valdarnini 1991; Plionis et al 1993). These studies have shown that the cause of the deep dipole contributions should be attributed mostly to the Shapley concentration, a huge mass overdensity located at  $\sim 140 h^{-1}$  Mpc in the general direction of the Hydra-Centaurus supercluster

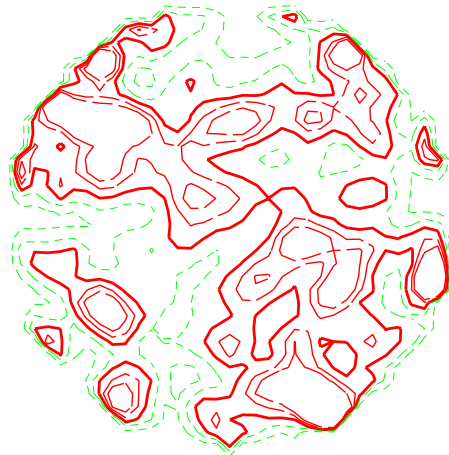


**Figure 5.** Contour plot of the smoothed 1.2 Jy IRAS galaxy distribution in real space and on the supergalactic plane.

(Shapley 1930; Scaramella et al 1989; Raychaudhury 1989).

To investigate further the possible cause of the present IRAS dipole results we have smoothed the IRAS 1.2 Jy galaxy distribution in a  $40^3$  cube with a cell size of  $10 h^{-1}$  Mpc using a Gaussian with smoothing radius equal to one cell and weighting each galaxy by  $\phi^{-1}$ . Due to the coupling between the selection function and the constant radius smoothing, we correct the resulting smoothed distribution for a distance dependent effect, which we quantified using N-body simulations (details will be presented in a forthcoming paper). In figure 5 we present the smoothed IRAS 1.2 Jy galaxy distribution on the supergalactic plane (of  $10 h^{-1}$  Mpc width) within  $170 h^{-1}$  Mpc. The contour step is 0.4 in overdensity while the  $\delta\rho/\rho = 0$  level appears as a thick continuous line.

Well known structures appear in this plot; the largest and most evident is the Shapley concentration located at  $(X_{sup}, Y_{sup}) \approx (-120, 60)$ , the Perseus-Pisces supercluster at  $(X_{sup}, Y_{sup}) \approx (60, -40)$ , the Coma supercluster at  $(X_{sup}, Y_{sup}) \approx (-20, 70)$ , the Ursa-Major supercluster at  $(X_{sup}, Y_{sup}) \approx (100, 100)$ , the Pisces-Cetus supercluster at  $(X_{sup}, Y_{sup}) \approx (50, -140)$  while the Great Attractor (Hydra-Centaurus complex ?), at  $(X_{sup}, Y_{sup}) \approx (-30, 30)$  appears in the foreground of the Shapley concentration. Furthermore, figure 5 is very similar to the corresponding Abell/ACO cluster density field (cf. Tully et al 1992; Branchini & Plionis 1996, their figure 3), and we therefore obtain a consistent picture, from both IRAS galaxy and Abell/ACO cluster data, in which the Shapley concentration is the most probable cause of the deep dipole contributions while the general alignment of the Great Attractor, Perseus-Pisces and

Shapley superclusters is most probably the cause of the apparent *coherence* of the IRAS galaxy dipole.

#### 4.4 $\Omega_{\circ}^{0.6}/b_I$ from the IRAS dipoles

Using the real-space dipole results and equation (3), we can estimate the density parameter  $\beta_{IRAS}$ . However, the value obtained should be considered rather as an upper limit since the deep contributions to the dipole, for which we do have strong indications, are probably not fully revealed by the present samples (see Kolokotronis et al 1996). Taking into account the scatter among the two IRAS samples, the amplitude variations at large depths and the uncertainties of the velocity model used to recover the real-space galaxy distances, we find:

$$\beta_{IRAS} \lesssim 0.78(\pm 0.1), \quad (9)$$

in agreement with the QDOT analysis of Rowan-Robinson et al (1990) but slightly larger, although within  $1\sigma$ , than the 1.2 Jy results of Strauss et al (1992). This value of  $\beta_I$  implies either that  $\Omega_{\circ} \lesssim 0.66$  for  $b_{IRAS} = 1$  or  $\Omega_{\circ} \simeq 1$  for  $b_{IRAS} \gtrsim 1.28$ .

## 5 CONCLUSIONS

Using a consistent analysis procedure we find that within  $50 h^{-1}$  Mpc, both the 1.2Jy and 0.6Jy (QDOT) IRAS samples, give identical dipole results while beyond this depth the QDOT dipole increases substantially up to  $100 h^{-1}$  Mpc, in agreement with Rowan-Robinson et al (1990). Furthermore there are significant indications for (a) dipole contributions from depths  $\sim 170 h^{-1}$  Mpc, in agreement with other recent large-scale studies (cf. Plionis & Kolokotronis 1998) and (b) a coherence of the dipole anisotropy extending to similar depths. The most probable cause of these deep dipole contributions is the Shapley mass concentration, while of the dipole *coherence* is the general alignment, on the supergalactic plane, of the Perseus-Pisces supercluster, the Great Attractor and the Shapley concentration, which span a range of  $\sim 200 h^{-1}$  Mpc.

A similar study of the complete (6 in 6) IRAS 0.6 Jy sample (PSCz) should give better indications of these results, although the overall amplitude of the effect could be probably estimated by a deeper catalogue (limited at a lower flux limit).

## ACKNOWLEDGEMENTS

We thank Enzo Branchini for providing us with the reconstructed IRAS 1.2 Jy galaxy peculiar velocities.

## REFERENCES

Branchini E., Plionis M., 1996, ApJ, 460, 569

- Branchini E., Plionis M., Sciamia D.W., 1996, ApJ, 461, L17  
 Dekel A., 1994, ARA&A, 32, 371  
 Dekel A., 1997, in L.da Costa ed. 'Galaxy Scaling Relations: Origins, Evolution & Applications', Springer, in press  
 Fisher, K.B., Huchra, J.P., Strauss, M.A., Davis, M., Yahil, A. & Schlegel, D., 1995, ApJS, 100, 69  
 Hudson M.J., 1993, MNRAS, 265, 72  
 Kaiser N., 1984, ApJ, 284, L9  
 Kaiser N., 1987, MNRAS, 227, 1  
 Kogut et al, 1993, ApJ, 419, 1  
 Kolokotronis, V., Plionis, M., Coles, P., Borgani, S., Moscardini, L., 1996, MNRAS, 280, 186  
 Lahav O., 1987, MNRAS, 225, 213  
 Lauer T.R. & Postman, M., 1994, ApJ, 425, 418  
 Lynden-Bell, D., Faber, S.M., Burstein, D., Davies, R.L., Dressler, A., Terlevich, R.J. & Wegner, G. 1988, ApJ, 326, 19  
 Lynden-Bell, D., Lahav O. & Burstein, D., 1989, MNRAS, 241, 325  
 Miyaji T., Boldt E., 1990, ApJ, 353, L3  
 Peebles, P.J.E., 1988, ApJ, 332, 17  
 Peebles P.J.E., 1980. The Large Scale Structure of the Universe, Princeton University Press, Princeton New Jersey  
 Plionis, M. & Valdarnini, R., 1991, MNRAS, 249, 46  
 Plionis M., Coles P., Catelan P., 1993, MNRAS, 262, 465  
 Plionis M. & Kolokotronis, V., 1998, ApJ, 500, June 10<sup>th</sup> issue.  
 Rowan-Robinson M., Lawrence A., Saunders W., Crawford J., Ellis R.S., Frenk C.S., Parry I., Xiaoyang X., Allington-Smith J., Efstathiou G., Kaiser N., 1990, MNRAS, 247, 1  
 Raychaudhury, S. 1990, Nat., 342, 251  
 Saunders W., Rowan-Robinson M., Lawrence A., Efstathiou G., Kaiser N., Ellis R.S. & Frenk, C.S., 1990, MNRAS, 242, 318  
 Scaramella, R., Vettolani, G., Zamorani, G., 1991, ApJ, 376, L1  
 Scaramella, R., Baiesi-Pillastrini, G., Chincarini, G., Vettolani, G. & Zamorani, G. 1989, Nat., 338, 562  
 Shapley, H. 1930, Harvard Obs. Bull., 874, 9  
 Strauss M.A. & Willick, J.A. 1995, Phys. Rep., 261, 271  
 Strauss M.A., Yahil A., Davis M., Huchra J.P., Fisher K., 1992 ApJ, 397, 395  
 Tully, R.B., Scaramella, R., Vettolani, G. & Zamorani, G., 1992, ApJ, 388, 9  
 Yahil A., Walker, D., Rowan-Robinson, M., 1986, ApJ, 301, L1  
 Yahil A., Strauss M., Davis M., Huchra J.P., 1991, ApJ, 372, 380